

Low energy (e, 2e) study from the 1t₂ orbital of CH₄

S. Xu, Hari Chaluvadi, X. Ren, T. Pflüger, A. Senftleben et al.

Citation: *J. Chem. Phys.* **137**, 024301 (2012); doi: 10.1063/1.4732539

View online: <http://dx.doi.org/10.1063/1.4732539>

View Table of Contents: <http://jcp.aip.org/resource/1/JCPSA6/v137/i2>

Published by the American Institute of Physics.

Additional information on J. Chem. Phys.


Journal Homepage: <http://jcp.aip.org/>

Journal Information: http://jcp.aip.org/about/about_the_journal

Top downloads: http://jcp.aip.org/features/most_downloaded

Information for Authors: <http://jcp.aip.org/authors>

ADVERTISEMENT



AIPAdvances

Special Topic Section:
PHYSICS OF CANCER

Why cancer? Why physics? [View Articles Now](#)

Low energy (e, 2e) study from the $1t_2$ orbital of CH_4

S. Xu,^{1,2} Hari Chaluvasi,³ X. Ren,² T. Pflüger,² A. Senftleben,² C. G. Ning,⁴ S. Yan,¹ P. Zhang,¹ J. Yang,¹ X. Ma,^{1,a)} J. Ullrich,^{2,5} D. H. Madison,^{3,b)} and A. Dorn^{2,c)}

¹Institute of Modern Physics, Chinese Academy of Sciences, Lanzhou 730000, China

²Max-Planck-Institut für Kernphysik, Saupfercheckweg 1, 69117 Heidelberg, Germany

³Department of Physics, Missouri University of Science and Technology, Rolla, Missouri 65409, USA

⁴Department of Physics and State Key Laboratory of Low-Dimensional Quantum Physics, Tsinghua University, Beijing 100084, China

⁵Physikalisch-Technische Bundesanstalt, Bundesallee 100, 38116 Braunschweig, Germany

(Received 2 May 2012; accepted 18 June 2012; published online 9 July 2012)

Single ionization of the methane (CH_4) $1t_2$ orbital by 54 eV electron impact has been studied experimentally and theoretically. The measured triple differential cross sections cover nearly a 4π solid angle for the emission of low energy electrons and a range of projectile scattering angles. Experimental data are compared with theoretical calculations from the distorted wave Born approximation and the molecular three-body distorted wave models. It is found that theory can give a proper description of the main features of experimental cross section only at smaller scattering angles. For larger scattering angles, significant discrepancies between experiment and theory are observed. The importance of the strength of nuclear scattering from the H-nuclei was theoretically tested by reducing the distance between the carbon nuclei and the hydrogen nuclei and improved agreement with experiment was found for both the scattering plane and the perpendicular plane. © 2012 American Institute of Physics. [<http://dx.doi.org/10.1063/1.4732539>]

I. INTRODUCTION

Electron impact single ionization of atomic and molecular targets is a fundamental process which is important in a wide range of science and technology, such as plasmas physics, chemistry of planetary atmospheres, and radiation damage of living tissues. Detailed information about this process can be obtained from the kinematically complete experiments, or (e, 2e) experiments, which determine the momentum vectors of all continuum particles (i.e., initial state of the projectile electron and the two final state electrons after ionization). From such measurements, triple differential cross sections (TDCSs) can be deduced to provide the most rigorous test of theoretical models.

Previous (e, 2e) studies about the collision dynamics mainly focused on atomic targets,^{1–5} and works dedicated to the molecular targets are scarce because of difficulties in both experiment and theory. On the experimental side, the closely spaced electronic states of molecules are difficult to be resolved.^{6–10} On the theoretical side, the multi-center nature makes calculations more complicated compared to atomic targets. In addition, the target molecules are randomly oriented in most of the experiments, thus theoretical results need to be averaged over all the possible orientations to allow comparison with experiment.⁷ In spite of such challenges, different molecules such as H_2 ,^{11,12} N_2 ,^{13–15} H_2O ,^{16–18} CO_2 ¹⁹ have been studied experimentally, and several theoretical models, such as the Brauner, Briggs, and Klar (BBK) model,⁷ the time

dependent close coupling (TDCC) model,^{20,21} and the molecular 3-body distorted wave (M3DW) model^{6,8,10,22,23} coupled with the orientation-averaged molecular orbital approximation (OAMO),²⁴ have been adapted to molecular targets.

Most of the previous (e, 2e) experiments were performed under the so-called coplanar asymmetric geometry, in which the energy and angular location of the scattered electron are fixed, and the emitted electron is detected in the scattering plane defined by the momentum vectors of the projectile and scattered electron. Binary and recoil peaks are found to be the dominant features in the cross sections for all atomic and molecular targets in a wide projectile energy range. Good agreement between theory and experiment has been achieved for atomic targets, especially for the simplest atoms such as H (Refs. 1 and 2) and He.^{3,4} However, for molecular targets, there are some difficulties for theory to reproduce the most basic features, such as the relative size of the recoil to the binary peak. Lohmann and co-workers measured the TDCSs for single ionization of different orbitals of H_2O by 250 eV electron impact and observed very large recoil peaks.¹⁶ These were well reproduced by the BBK model in a later publication.¹⁷ To further examine the BBK theory, Lahmam-Bennani and co-workers applied the BBK model to single ionization of CH_4 with incident electron energy around 600 eV. They found that the experimental TDCSs exhibited again a large recoil peak which was not reproduced by BBK theory.⁷ The authors attributed the large recoil scattering to the particular kinematics under which the electron-nucleus interaction is strong, but such interaction is not properly considered in the BBK theory. Toth and Nagy⁹ showed that a strong electron-nucleus interaction can be simulated by localizing the H-nuclei closer to the center of mass in their spherical shell approximation of the

a) Author to whom correspondence should be addressed. Electronic mail: x.ma@impcas.ac.cn.

b) madison@mst.edu.

c) dornalex@mpi-hd.mpg.de.

nuclear potential, and good agreement with experiment was achieved.⁹ Such method was then adopted to N_2 in a recent publication.¹⁵ The calculation agrees well with experiment for outer molecular orbitals, but cannot reproduce the large recoil peak for the inner $2\sigma_g$ orbital. In a recent study on H_2 it was shown both experimentally and theoretically that shortening the internuclear distance increases the binding potential and, hence, the relative contribution of recoil scattering.²⁵

The M3DW is a model that has been widely employed in (e, 2e) studies for various molecular targets under different kinematics. A review of this work is contained in Ref. 22. Lohmann and co-workers measured the TDCSs for the complex CHOOH (Ref. 6) and tetrahydrofuran⁸ targets, and compared their results with M3DW calculations. The measurement showed that for the emitted electron energy of 10 eV, the relative size of the recoil to the binary peak decreases as the scattering angle increases, and is much smaller than that observed in ionization of water under similar kinematics. The authors attributed these to the special molecular configurations of the two targets. For both targets, there is no nucleus at the center-of-mass, which suggests that the electron-nuclei interaction might not be as strong as that for molecules with nuclei located at/around the center-of-mass, such as H_2O . However, since the same trend of the relative size of the recoil to the binary peak is observed for ionization of the outmost orbitals of single center atomic targets He,⁴ Ne,⁵ and Xe (Ref. 5) under similar kinematics, this may indicate that the nuclear configuration is not the only/dominant cause of this phenomenon. The M3DW calculation agrees well with the experiment for large scattering angles where the recoil peak is small, but does not reproduce the large recoil peak for small scattering angles.

Recently, Nixon *et al.*¹⁰ performed low energy (e, 2e) studies of CH_4 for the symmetric coplanar geometry. For ionization of the $1t_2$ state, the location of the small angle peak and the relative sizes of the small and large angle peaks were qualitatively reproduced by the M3DW, but the theory predicted the large angle peak at smaller angles than observed in experiment. For ionization of the $2a_1$ state, the M3DW was in better agreement with experiment for high energies than low energies and for low energies experiment found 3 peaks while theory only had 2 peaks. They also compared ionization of the $2a_1$ state of CH_4 with the $2s$ state of neon. For neon, there was excellent agreement between experiment and theory for high energy while for low energy experiment found more peaks than theory similar to the methane $2a_1$ results. This suggests that the molecular nature of the target is not the only cause of the disagreement between theory and experiment, and that the nuclear scattering may also play a dominant role that is not being properly treated.

There are also some experiments that have been performed for out-of-plane geometries. For example, Al-Hagan and co-workers analyzed the cross section for the geometry where both final state electrons are emitted in the plane perpendicular to the incoming beam.¹² The TDCSs in this geometry exhibited different features for the isoelectronic targets He and H_2 . A strong peak for back-to-back emission of electrons was observed for He, while a minimum was observed for H_2 . The authors introduced a multi-scattering process to

explain such difference. The origination of the difference was attributed to different nuclear configurations of the two center H_2 molecule and the one center He atom. The authors concluded that all the molecules with a nucleus in the center-of-mass, such as CH_4 , should behave in a similar way as He. However, a recent study²³ showed that this prediction failed for the isoelectronic targets Ne and CH_4 which are more complicated than the targets discussed in Ref. 12. Ren *et al.* measured the 3D TDCSs for He and H_2 using the reaction microscope. Their study showed that the strong back-to-back emission of two outgoing electrons for (e, 2e) of He is mainly due to the overlap of the binary and recoil lobes.²⁶

In short, previous (e, 2e) studies show that the molecular configurations of the targets influence the features of the TDCSs in both the coplanar and out-of-plane geometries. CH_4 is the simplest hydrocarbon molecule present in nature. It is a benchmark molecule with a nucleus at the center-of-mass. Thus, electron- CH_4 collisions represent an ideal system to investigate the influence of molecular configurations on the electron emission patterns in the (e, 2e) process.

In this paper, we explore single ionization of the $1t_2$ orbital of CH_4 by 54 eV electron impact. By employing the advanced reaction microscope technique, TDCSs under different geometries were measured and compared with M3DW and DWBA calculations.

II. EXPERIMENT

A. Experimental apparatus

The experiment was performed with a reaction microscope that was specially designed for (e, 2e) studies. Details of the experimental procedure were given in previous publications.^{27,28} In brief, a pulsed electron beam with energy of 54 eV crosses the CH_4 supersonic gas jet, and causes single ionization of the target. Using the uniform electric and magnetic fields, the charged fragments in the final state are extracted and directed to the two individual time and position sensitive detectors. In this way, a large part of the 4π solid angle is covered for final state particles (100% for the detection of CH_4^+ ions and 80% for electrons with energy lower than 20 eV). The momentum components of the recoil ion and the electrons along the projectile direction (longitudinal components) can be determined from the time of flight of each particle from the collision region to the respective detector, while the transverse momentum can be obtained from the position and the time of flight information recorded by the detectors. For recoil ions, since the so-called time-focusing condition^{28,29} is employed in the spectrometer, the longitudinal momentum has a much higher resolution (0.4 a.u.) compared to the transverse component (1.2 a.u.). It should be emphasized that the TDCSs are deduced directly from the momenta of the two outgoing electrons without relying on the recoil ion momentum, thus the angular resolution is not influenced by the temperature of the heavy target. Experimentally, a large range of the final state phase space is recorded simultaneously. Thus, in the offline data analysis particular scattering geometries of interest are selected by choosing those events which fulfill particular conditions

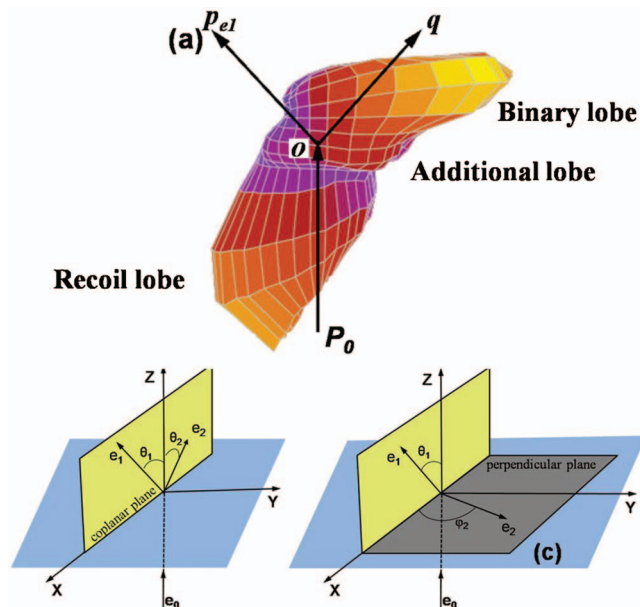


FIG. 1. (a) TDCS for $(e, 2e)$ of $1t_2$ orbital of CH_4 as a function of the emission angle of the slow electron with kinetic energy of $E_2 = 10$ eV. The scattering angle of the faster electron is fixed to $\theta_1 = -55^\circ$; (b) and (c): coplanar and perpendicular plane geometries used for the present studies. See text for details.

concerning, e.g., the faster electron scattering angle or the energy partitioning between both electrons in the final state. The resolution for obtaining the target electron binding energy is around 6 eV during the present experiment. Since the CH_4^+ ion is only produced from the $(1t_2)^{-1}$ state,³⁰ the contribution from the higher ionization/ionization-excitation states can be well separated from $(1t_2)^{-1}$ by coincidence measurement of the CH_4^+ ion. It should, however, be noted that ionization from the $(1t_2)$ orbital can yield other fragments as well that have not been studied in this work.

B. Definition of geometries

Figure 1(a) is an example of the measured three-dimensional (3D) polar plot of the TDCS for single ionization of the $1t_2$ orbital of CH_4 . The scattering angle of the faster electron is fixed at $\theta_1 = 55^\circ$, while the emission angle of the slow electron with energy 10 eV covers a large range of the full 4π solid angle. In such diagrams, the TDCS for emission to a particular direction is proportional to the distance between the origin and the point on the surface of the 3D plot intersected by the electron's emission direction. In order to get a reduced scattering of the data points in this 3D plot, the count in each unit is summed with the neighboring units. The cross section pattern is dominated by the binary and recoil lobes which are universal in the $(e, 2e)$ process. An additional structure is observed between the binary and recoil lobes. This lobe may arise from high-order effects which would be particularly important at low incident energy.¹⁰

To make a more quantitative comparison between experiment and theory, we define two different geometries, the coplanar geometry shown in Figure 1(b) and the perpendicular plane geometry in Figure 1(c). The energy (E_1) and scatter-

ing angle of the scattered (faster) electron (θ_1) and the energy of the emitted (slower) electron (E_2) are fixed for both geometries. For the coplanar geometry in Figure 1(b), the slow electron is detected in the scattering plane defined by the momenta of the fast scattered electron and the incident projectile. The TDCS is given as a function of the scattering angle of the slow electron (θ_2) measured clockwise relative to the incident beam direction. For the perpendicular plane geometry in Figure 1(c), the slow electron is detected in the plane perpendicular to the incident electron beam. The TDCS is plotted as a function of the angle (φ_2) between the momentum vector of the slow electron and the projection of the faster electron momentum onto the perpendicular plane. The intersection of the two planes corresponds to $\theta_2 = 90^\circ (270^\circ)$ in the coplanar plane, and $\varphi_2 = 180^\circ (0^\circ)$ in the perpendicular plane. For both geometries, the cross sections are integrated over an angular range of $\pm 10^\circ$ above and below the defined plane.

III. THEORETICAL FRAMEWORK

The molecular M3DW approximation has been presented in previous publications^{31,32} so only a brief outline of the theory will be presented. The TDCS for the M3DW is giving by

$$\frac{d\sigma}{d\Omega_a d\Omega_b dE_b} = \frac{1}{(2\pi)^5} \frac{k_a k_b}{k_i} (|T_{dir}|^2 + |T_{exc}|^2 + |T_{dir} - T_{exc}|^2), \quad (1)$$

where \vec{k}_i , \vec{k}_a , and \vec{k}_b are the wave vectors for the initial, scattered and ejected electrons, T_{dir} is the direct scattering amplitude, and T_{exc} is the exchange amplitude. The direct scattering amplitude is given by

$$T_{dir} = \langle \chi_a^-(\vec{k}_a, \mathbf{r}_1) \chi_b^-(\vec{k}_b, \mathbf{r}_2) C_{scat-eject}(\mathbf{r}_{12}^{ave}) | V - U_i | \phi_{DY}^{OA}(\mathbf{r}_2) \chi_i^+(\vec{k}_i, \mathbf{r}_1) \rangle, \quad (2)$$

where r_1 and r_2 are the coordinates of the incident and the bound electrons, χ_i , χ_a , and χ_b are the distorted waves for the incident, scattered, and ejected electrons, respectively, and $\phi_{DY}^{OA}(\mathbf{r}_2)$ is the initial bound-state Dyson molecular orbital averaged over all orientations. The molecular wave functions were calculated using density functional theory along with the standard hybrid B3LYP (Ref. 33) functional by means of the ADF 2007 (Amsterdam density functional) program³⁴ with the TZ2P (triple-zeta with two polarization functions) Slater type basis sets. For the $1t_2$ state, the average of the absolute value of the Dyson wave-function is taken prior to the collision since the normal average is zero due to parity of the wave-function.¹⁰ The factor $C_{scat-eject}(\mathbf{r}_{12}^{ave})$ is the Ward-Macek average Coulomb-distortion factor between the two final state electrons,³⁵ V is the initial state interaction potential between the incident electron and the neutral molecule, and U_i is a spherically symmetric distorting potential which is used to calculate the initial-state distorted wave for the incident electron $\chi_i^+(\vec{k}_i, \mathbf{r}_1)$. For the exchange amplitude T_{exc} , particles 1 and 2 are interchanged in the final state wavefunction (left-hand side) in Eq. (2).

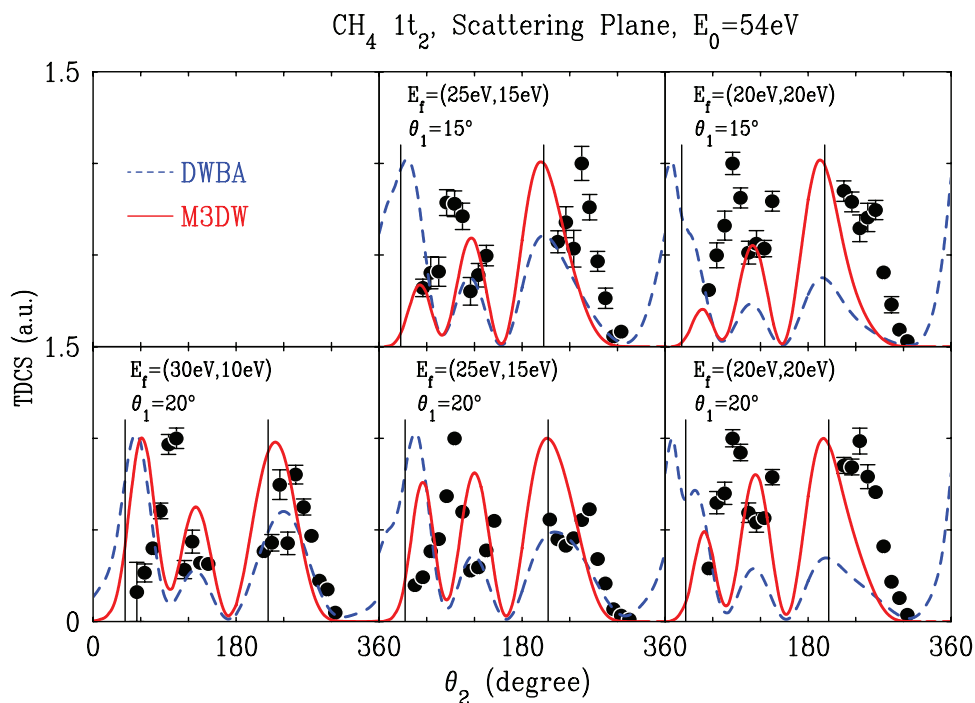


FIG. 2. TDCSs for the scattering plane geometry. The emission angle of the faster final state (scattered) electron is 15° and 20° , while the emitted electron energy ranges between 10 eV and 20 eV. The experimental data are the black circles and the theoretical results are the DWBA (dashed curve) and M3DW (solid curve). The horizontal axis is the observation angle for the slower (ejected) electron. The vertical line at small ejection angles is the direction of classical momentum transfer and the vertical line at larger ejection angles is the direction of the classical recoil peak. The experimental and theoretical data have been normalized to unity independently at the maximum for each curve.

The Schrödinger equation for the incoming electron wave-function is given by

$$\left(T + U_i - \frac{k_i^2}{2}\right) \chi_i^+(\vec{k}_i, r) = 0, \quad (3)$$

where T is the kinetic energy operator and the “+” superscript on $\chi_i^+(\vec{k}_i, r)$ indicates outgoing wave boundary conditions. The initial state distorting potential contains three components $U_i = U_s + U_E + U_{CP}$, where U_s contains the nuclear contribution plus a spherically symmetric approximation for the interaction between the projectile electron and the target electrons which is obtained from the quantum mechanical charge density of the target. The nuclear contribution to U_s consists of a charge of +6 at the center of mass and a charge of +4 located on a thin spherical shell at the equilibrium distance of 2.06 a.u. relative to the center of mass. U_E is the exchange potential of Furness-McCarthy (corrected for sign errors)³⁶ which approximates the effect of the continuum electron exchanging with the passive bound electrons in the molecule, and U_{CP} is the correlation-polarization potential of Perdew and Zunger.^{37,38}

The final state for the system is approximated as a product of distorted waves for the two continuum electrons times the average Coulomb-distortion factor. The final state distorted waves are calculated as for the initial state except that the final state spherically symmetric static distorting potential for the molecular ion is used for U_s .

Results will be presented for the M3DW described above as well as the standard distorted wave Born approximation (DWBA). The DWBA is identical to the M3DW except that

the post collision interaction (PCI) term $C_{scat-eject}(r_{12}^{ave})$ is omitted in the evaluation of the direct and exchange amplitudes.

IV. RESULTS AND DISCUSSION

A. TDCSs under coplanar geometry

Since the ionization energy for the $1t_2$ state is 14 eV, the two final state electrons have 40 eV to share when the incident electron has energy of 54 eV. Several energy pairs (E_1, E_2) were analyzed where E_1 is the energy of the faster electron and E_2 the slower with $E_1 + E_2 = 40$ eV. For each energy pair, different scattering angles θ_1 of the fast final state electron were selected ranging from 15° to 55° . Figure 2 compares theoretical and experimental coplanar results for three different energy pairs and faster electron scattering angles of 15° and 20° .

The experimental data exhibit the normal binary peak at small angles and recoil peak at large angles. The vertical line on each figure at small scattering angles indicates the classical momentum transfer direction and the line at large angles is the location of the classical recoil direction (i.e., the opposite of the momentum transfer direction). Since the ionized $1t_2$ orbital has p -character with a minimum of the bound momentum wave function at zero momentum, the binary peak can show a split structure with two maxima when the reaction kinematics is close to the region of the Bethe ridge. It is possible that the observed splits of the binary peaks in both the experimental data and the theoretical curves are due to the p -character of the $1t_2$ orbital. This has been

seen for higher incident electron energies for ionization of $2p$ state of Ne.³⁹ However, for the atomic case, the double peaks become a single peak as the incident electron energy is lowered to those of the present experiment³⁹ due to the enhanced influence of high order effects. In Sec. IV C, we will show that the second binary peak is suppressed when scattering from the nuclei is made stronger. So this peak may be more strongly related to nuclear scattering than the $2p$ structure of the molecular wavefunctions. At higher incident-electron energies, one would expect that the binary peak should be close to the momentum transfer direction and the recoil peak should be close to the opposite direction. For the low energies considered in this work, it is seen that the experimental binary peak is significantly shifted to larger angles. In principle, this could be the result of the PCI between the ejected electron and the scattered electron which in the diagrams in Figure 2 is fixed at the angle $(360^\circ - \theta_1)$. The precise position of the recoil peak cannot be well judged since it is only partly in the experimentally accessible angular range. Nevertheless, while theory predicts recoil peaks fairly well centered at the direction opposite to the momentum transfer, the experimental recoil lobes extend to larger angles, in particular, for equal energy sharing of the final state electrons.

Some information on the mechanisms underlying the experimental cross section patterns can be gained from compar-

ison with theory. Both calculations show a significant shift of the binary peaks away from the momentum transfer direction. Although the DWBA does not contain PCI directly in the T-matrix, the phenomenon is indirectly taken into account by the distorted wave description, i.e., the higher order projectile target interactions in the initial and final states must play a key role for this shift. The comparison with the M3DW calculation, which contains PCI directly in the T-matrix, shows that the role of PCI is a suppression of the cross section in the vicinity of the scattered projectile direction $(360^\circ - \theta_1)$. As expected this effect is weak for the most asymmetric energy sharing (30 eV, 10 eV), where the DWBA and M3DW results are similar in the momentum transfer direction. On the other hand, for equal energy sharing PCI is strong and gives rise to a significant reduction and a shift of the small angle binary peak while the magnitude of the large angle peak at about 120° is increasing. Experimentally the binary peaks are observed at even larger angles. Finally, both theories show the recoil peak at a position roughly opposite to momentum transfer direction and do not show the apparent shift of the experimental peaks to larger angles. The large magnitude of the recoil peak, which is similar in size to the binary peak in most cases is reproduced. The best overall agreement of experiment and theory is observed for the most asymmetric energy sharing case (30 eV, 10 eV) with $\theta_1 = 20^\circ$.

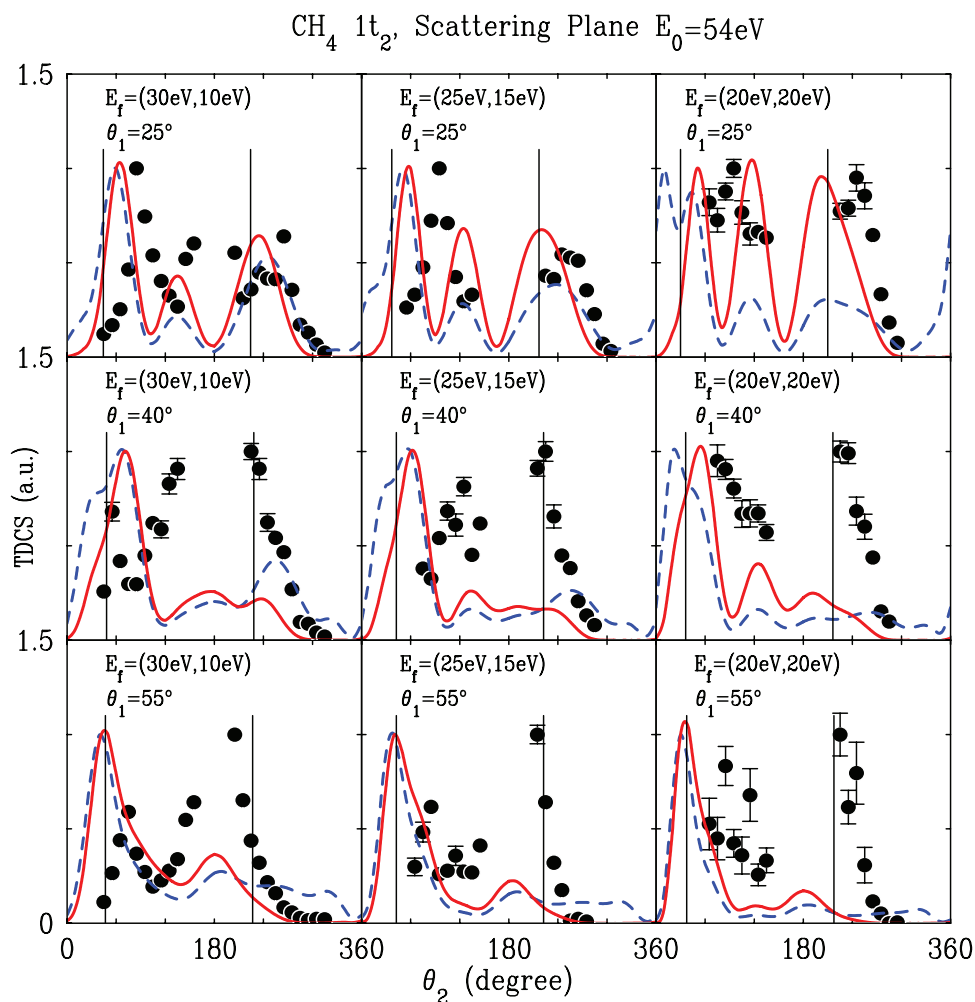


FIG. 3. Same as Figure 2 except for higher final state (scattered) electron angles of 25° , 40° , and 55° .

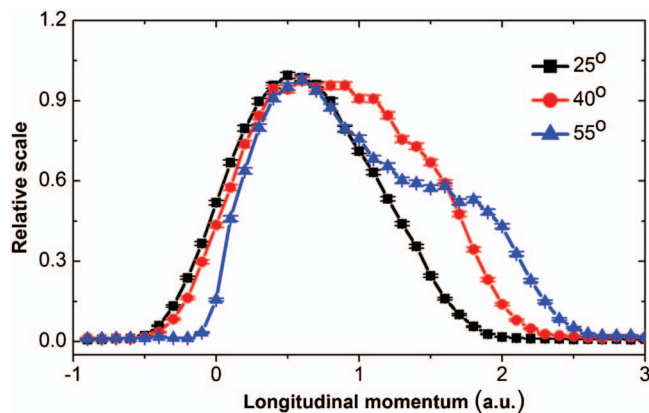


FIG. 4. Longitudinal momentum distributions at different scattering angles. The curves are integrated over all the emitted electron energy of e_2 .

Figure 3 contains the same comparison between experiment and theory for faster electron scattering angles of 25° , 40° , and 55° . For these larger scattering angles, the experimental TDCSs is still dominated by the binary and recoil peaks with the recoil peaks as large as or larger than the binary peaks. In a recent study on the low energy (e , $2e$) of Ar,⁴⁰ a new structure is observed in the projectile backwards direction. It is also possible that the peaks around 180° observed in the present study (e.g., for (30 eV, 10 eV) and $\theta_1 = 25^\circ$) originates from the same mechanisms. For the two

largest angles, the experimental recoil peaks are close to the classical recoil direction. With increasing θ_1 , the theoretical calculations evolve into a single binary peak very close to the classical binary direction. In Sec. IV C, we will show that the second binary peak is suppressed when scattering from the H-nuclei is made stronger. With increasing θ_1 , the projectile electron penetrates closer to the center of mass. Consequently, the reduction of the second binary peak seen here with increasing θ_1 is probably due to increased importance of nuclear scattering as a result of smaller impact collisions. Both the theoretical binary and recoil peaks occur at smaller angles than in experiment.

The recoil peak arises from a process in which the emitted electron produced by the binary collision is scattered backward by the nucleus. Thus the increased experimental recoil peak may be attributed to an increased interaction between the emitted electron and the target nuclei. While the emitted electron is scattered backward, momentum will be transferred to the recoil ion simultaneously. Consequently, the momentum distribution of the recoil ion provides direct information revealing how strong the electron-nuclei interaction is. As mentioned before, the advanced reaction microscope technique makes it possible to obtain the longitudinal momentum distribution of the recoil ions with a relative high resolution (0.4 a.u.). Figure 4 shows the longitudinal momentum distributions of the recoil ions at scattering angles of $\theta_1 = 25^\circ$, 40° , and 55° , respectively.

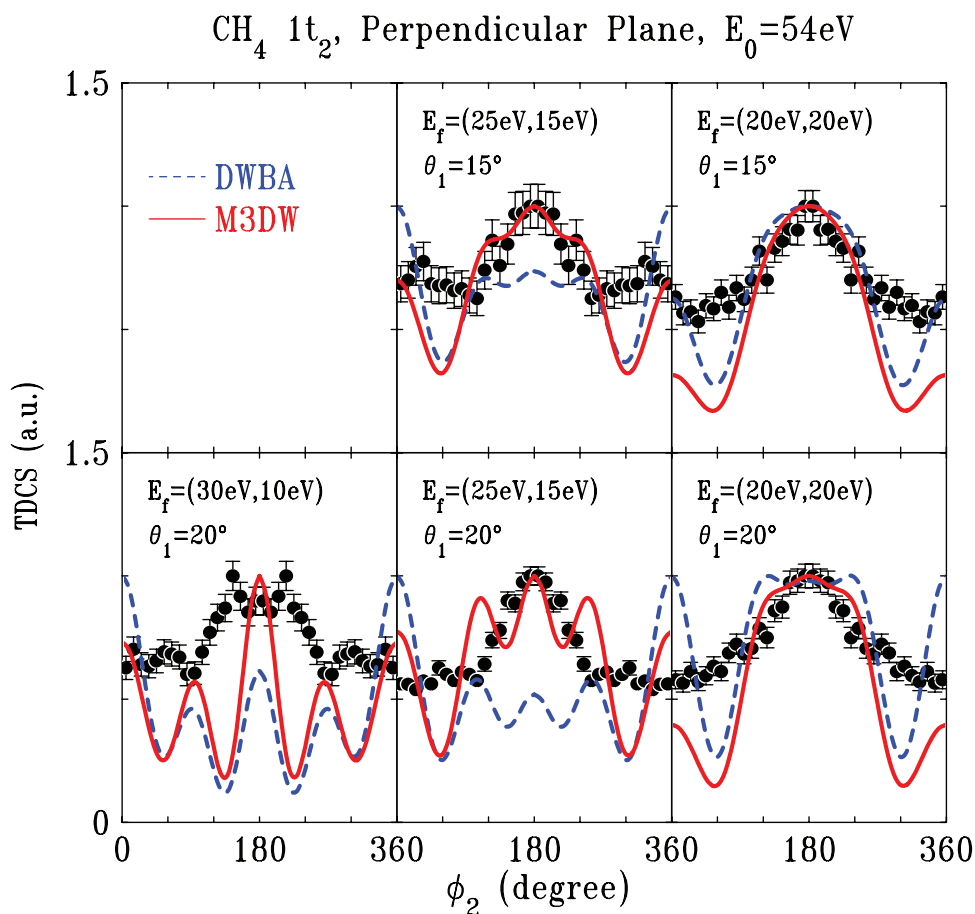


FIG. 5. Same as Figure 2 except for the perpendicular plane.

Figure 4 shows that, as the scattering angle increases, the longitudinal momentum distribution extends toward the larger momentum side (right-hand side), which indicates that the electron-nuclei interaction becomes stronger. In two recent studies for CHOOH (Ref. 6) and tetrahydrofuran,⁸ the relative size of the recoil to binary peak was found to decrease as the scattering angle increased. The authors suggested that this trend is due to the fact that there is no nucleus in/near the center-of-mass for both of these targets. For CH₄, the carbon nucleus is located at the center of the tetrahedron defined by the four protons. If we consider this process under the classical Rutherford scattering model, increasing the scattering angle indicates that the impact parameter of this collision process reduces, which means that the binary collision happens closer to the carbon nucleus. Thus, it stands to reason that the interactions between the target nuclei and the electrons should increase.

Finally, it can be concluded that increasing the relative size of the recoil to the binary peak of the TDCS in the scattering plane is due to an increased electron-nuclei interaction as the scattering angle increases. However, there are no experimental TDCSs for the molecules without a nucleus in the center of mass (for example N₂) under the same kinematics available for comparison. Consequently, it is hard to estimate from experiment how strong the molecular configuration influences the electron-nuclei interaction is.

Comparing with theory, the agreement tends to be better for small scattering angles, and it gets worse as the scattering angle increases in the scattering plane. This is consistent with the observations in Ref. 10, where better agreement was found for the forward peaks in the coplanar symmetric geometry employed in Ref. 10. These forward peaks correspond to small scattering angle events. For the backward peaks, which correspond to the events with larger scattering angle

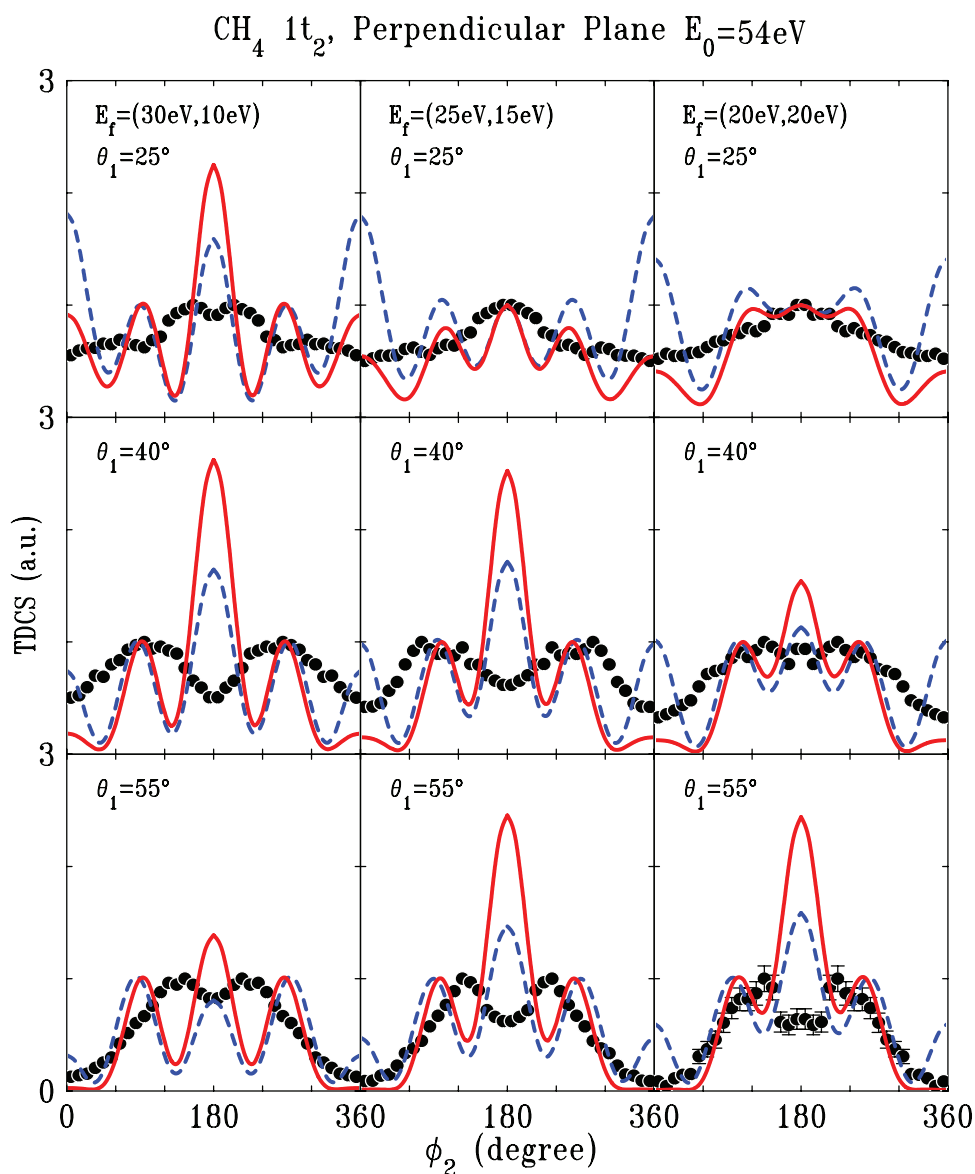


FIG. 6. Same as Figure 3 except for the perpendicular plane.

and stronger nuclei scattering, obvious discrepancy between theory and experiment is observed. Finally and on a more positive side, the present theoretical ratios of binary to recoil peak heights are reasonably good for scattering angles out to $\theta_1 = 25^\circ$.

B. TDCSs under perpendicular geometry

The collision dynamics at low incident energies are far away from the impulsive regime and higher order effects are expected to be important. Since the TDCS in the coplanar plane is dominated by the binary and recoil lobes, out-of-plane geometries such as the perpendicular plane defined in part II are good choices for investigation of higher order contributions. Figure 5 shows the TDCSs in the perpendicular plane with same kinematics as in Figure 2. The cross sections should be symmetrical about 180° . However, in some cases the experimental TDCSs show a deviation of around 10% between the equivalent points, which seems to be a systematic effect with the experiment. The data have been averaged for equivalent points to make a more effective comparison with calculations. It can be seen from Figure 5 that the experimental cross section has a maximum for 180° emission an-

gle which corresponds to the ejected electron being emitted in the scattering plane on the opposite side of the beam direction as the scattered electron and a minimum for 0° (360°) which corresponds to the ejected electron being emitted in the scattering plane on the same side of the beam direction as the scattered electron. The M3DW theoretical calculations also predict a maximum for 180° scattering but with more structure than seen in the data. The M3DW results are in better agreement with experiment than the DWBA and the DWBA tends to predict cross sections that are too large for 0° (360°).

Figure 6 shows the TDCSs in the perpendicular plane with the same kinematics as in Figure 3. There is very little structure in the experimental data except that the 180° maximum turns into a shallow minimum with increasing faster electron scattering angle. The experimental data for $\theta_1 = 55^\circ$ is very reminiscent of the Al-Hagan *et al.* results for ionization of H_2 with both final state electrons being detected in the perpendicular plane (i.e., $\theta_1 = 90^\circ$).¹² In that work, results for ionization of H_2 were compared with the equivalent cross sections for ionization of He. For H_2 , peaks were found near 90° and 270° and a minimum was found for 180° scattering. For He, peaks were found for angles in the vicinity of 90° and 270° as well as 180° . It was shown in that work that the 90° and 270° peaks resulted from elastic scattering into the

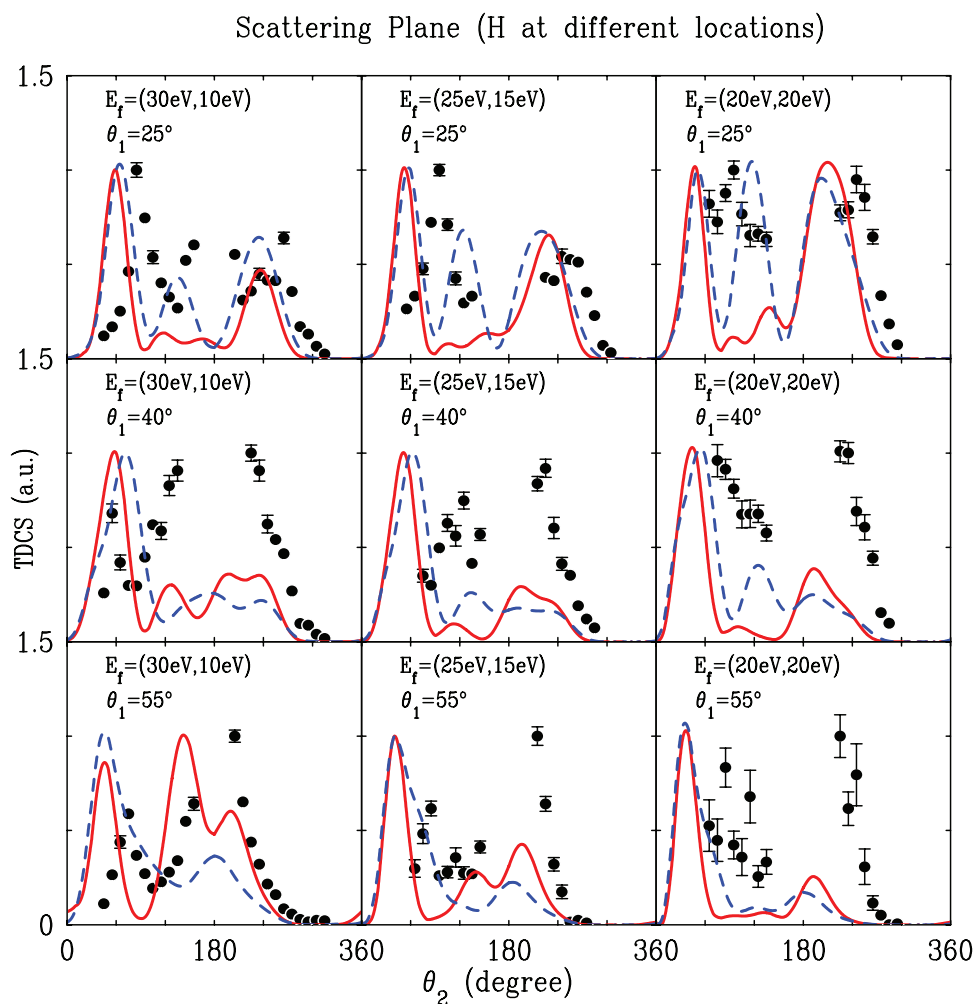


FIG. 7. Same as Figure 3 except for different theoretical curves. The theoretical results are the M3DW with the H-nuclei 2.06 a.u. from the C nucleus (dashed curve) and M3DW with the H-nuclei 0.8 a.u. from the C nucleus (solid curve).

perpendicular plane followed by a binary collision in the perpendicular plane. The minimum at 180° for H_2 was attributed to very small impact parameter binary collisions taking place between the two nuclei where the average nuclear attraction would be zero. The strong maximum for He was attributed to the strong attraction resulting from small impact parameters with the nuclear charge located at the center of mass. Al-Hagan *et al.*¹² predicted that ionization of any molecule with a nucleus at the center of mass should have 3 peaks in the perpendicular plane at 90° , 180° , and 270° just like both theoretical calculations predict for the present case.

Very recently, Nixon *et al.*²³ published low energy TDCS for ionization of CH_4 and Ne where both final state electrons were detected in the perpendicular plane. In that work, the energy of the incident electron was varied and both final state electrons were detected with the same energy. Their experimental results for (20 eV, 20 eV) and $\theta_1 = 90^\circ$ is very similar to the present results for (20 eV, 20 eV) and $\theta_1 = 55^\circ$ of Figure 6. Likewise, the theoretical DWBA and M3DW re-

sults presented in that work are similar to the results shown in Figure 6 with three peaks near 90° , 180° , and 270° as predicted by Al-Hagan *et al.*¹² but not found in the experiment. For electron energies above about 12 eV, Nixon *et al.*²³ found two peaks near 90° and 270° similar to the two peaks found in the present work for $\theta_1 = 40^\circ$, 55° and predicted by the theory. The intriguing question remains why both experiments find very little backscattering from the highly charged nucleus located at the center of mass while the theory predicts very strong backscattering.

C. The reduced C–H distance calculations

Toth and Nagy⁹ reported a DWBA calculation very similar to the present work for high energy ionization of CH_4 and compared their results with the coplanar experimental data of Lahman-Bennani *et al.*⁷ They noted that the standard DWBA predicted recoil lobes that were too small compared to experiment which they attributed to a weak scattering from

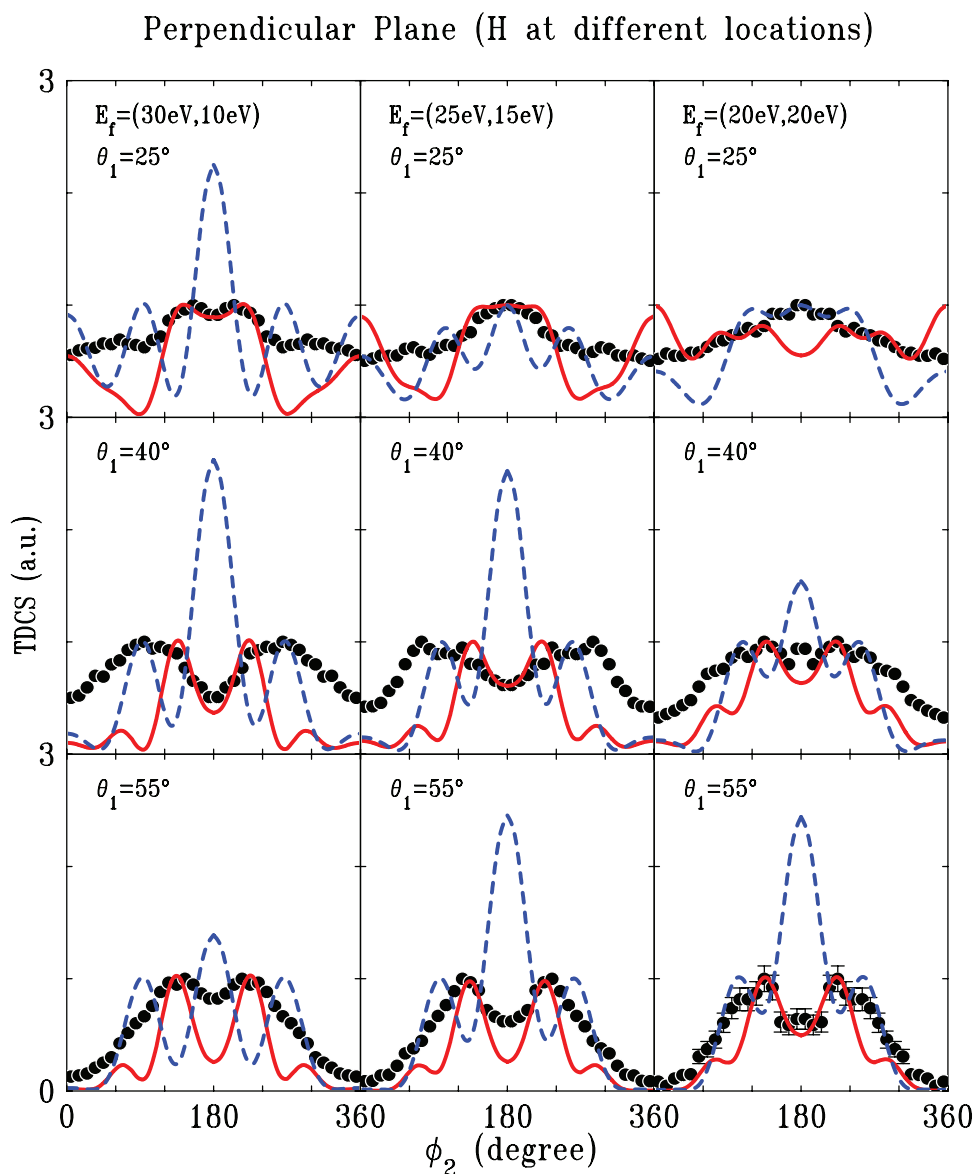


FIG. 8. Same as Figure 7 except for the perpendicular plane.

the H-nuclei. Recall that in the present spherically symmetric model, the four H-nuclei are uniformly distributed on a thin spherical shell of radius 2.06 a.u. They showed that, by decreasing this radius (and presumably increasing the strength of the attractive potential felt by the target electrons), they could increase the recoil lobe and achieve good agreement with experiment. Recently, an experimental verification of the increasing recoil contribution with decreasing inter-nuclear separation was found in molecular hydrogen.²⁵ Since the recoil lobes calculated with the H-shell radius of 2.06 a.u. for coplanar scattering and $\theta_1 = 40^\circ, 55^\circ$ are significantly smaller than experiment, we decided to try reducing the H radii to see if this would help. It is important to note that the electronic wavefunctions are not changed in these calculations. The only thing changed is the nuclear contribution to the distorting potential (i.e., the radius of the sphere with charge +4 is changed but everything else is unchanged).

Figure 7 shows the effect of reducing the H-shell radius to 0.8 a.u. for coplanar kinematics and the larger faster electron scattering angles presented in Figure 3. We found that, for coplanar scattering, the size of the sphere did not have a large effect on the ratio of binary to recoil lobes. The only important change from making the H-sphere smaller was to significantly reduce the right-hand side of the split binary peak to the point of essentially eliminating it. Although the results for the recoil peak are disappointing, they seem reasonable since the classical impact parameters for these scattering angles range between 5 and 11 a.u. such that a sphere of 2 a.u. looks the same as a point charge at the center classically. It is interesting to note that the second peak was suppressed by changing the strength of the scattering from the nuclei. Since the p-type wavefunctions were not changed in this calculation, these results suggest that the split lobe binary peak more closely related to nuclear scattering than the p-type structure of the wavefunction.

Although it would seem senseless to make the nuclear interaction stronger for the perpendicular plane since the present results indicate that the interaction with the nuclei is already too strong, we tried it anyway and the results are shown in Figure 8 for the larger scattering angles. Surprisingly, increasing the strength of the H-nuclear interaction changed the large backscattering peak to a minimum consistent with the experimental data. Now the agreement with experiment is not perfect but at least reasonable. Obviously the simple classical models are not able to explain this behavior and we are evidently seeing some kind of quantum interference effect. By using different size radii for different scattering angles, we could obtain even better agreement with experiment but we do not think that it is appropriate to push this model that far (it seems too much like curve fitting). On the other hand, since agreement with experiment was improved in both the scattering plane and perpendicular plane (contrary to expectation), we think that there may be some important physics contained herein. In any event, these results indicate that the cross sections are strongly dependent on the nuclear configuration. It is also imaginable that detecting electron ionization events coincident with the creation of a CH_4^+ ion selects ionization events that take place at certain nuclear geometries covered by the methane ground state nuclear wave

function. Other configurations will consequently lead to dissociation after removal of a $1t_2$ electron. The specific geometries leading to bound methane ions do not have to employ symmetrically arranged protons, i.e., the C–H bonds might have different lengths, as the ground state of the methane ion has a reduced symmetry due to Jahn-Teller distortions.⁴¹

V. CONCLUSIONS

Experimental (e, 2e) measurements for ionization of the $1t_2$ orbital of CH_4 induced by 54 eV electron-impact have been compared with DWBA and M3DW theoretical calculations. Up to a faster electron scattering angle of $\theta_1 = 25^\circ$ experiment and theory were in qualitative agreement concerning the relative magnitudes of the binary and recoil peaks. Remaining differences were the positions of the split binary peak and the recoil peak, which in experiment were observed at larger angles than predicted by theory. In the coplanar plane, the experimental relative size of the recoil peak to the binary peak increases as the scattering angle becomes larger while the theoretical recoil peak decreased in magnitude. Overall the agreement between experiment and theory was better for the smaller faster electron scattering angles. The importance of the strength of nuclear scattering from the H-nuclei was tested by reducing the distance between the carbon nuclei and the hydrogen nuclei and improved agreement with experiment was found for both the scattering plane and the perpendicular plane. This indicates that the averaging process of uniformly distributing a charge of +4 on a thin spherical shell unphysically dilutes the role of the hydrogen nuclei. The present study highlights the importance of the electron-nuclei interaction for the (e, 2e) process. Both the experimental and theoretical results exhibited a double binary peak which is seen for ionization of atomic $2p$ states at much higher incident electron energies. Increasing the strength of the scattering from the nuclei suppressed the second binary peak so the double binary peak seems to be more strongly related to nuclear scattering than the $2p$ structure of the molecular wavefunctions. Further experimental and theoretical works focusing on this issue are necessary.

ACKNOWLEDGMENTS

This work is partly supported by the U.S. National Science Foundation (NSF) under Grant No. PHY-1068237 and by the National Natural Science Foundation of China (NNSFC) under Grant Nos. 10979007, 10674140, and 10704046. S.X. is grateful for support from the CAS-MPS doctor training program, and helpful discussion from Dr. Toth and Professor Nagy.

¹T. N. Rescigno, M. Baertschy, W. A. Isaacs, and C. W. McCurdy, *Science* **286**, 2474 (1999).

²I. Bray, *Phys. Rev. Lett.* **89**, 273201 (2002).

³A. T. Stelbovics, I. Bray, D. V. Fursa, and K. Bartschat, *Phys. Rev. A* **71**, 052716 (2005).

⁴M. Dürr, C. Dimopoulou, A. Dorn, B. Najjari, I. Bray, D. V. Fursa, Z. Chen, D. H. Madison, K. Bartschat, and J. Ullrich, *J. Phys. B* **39**, 4097 (2006).

⁵M. A. Stevenson, L. R. Hargreaves, B. Lohmann, I. Bray, D. V. Fursa, K. Bartschat, and A. Kheifets, *Phys. Rev. A* **79**, 012709 (2009).

- ⁶C. J. Colyer, M. A. Stevenson, O. Al-Hagan, D. H. Madison, C. G. Ning, and B. Lohmann, *J. Phys. B* **42**, 235207 (2009).
- ⁷A. Lahmam-Bennani, A. Naja, E. M. Staicu Casagrande, N. Okumus, C. Dal Cappello, I. Charpentier, and S. Houamer, *J. Phys. B* **42**, 165201 (2009).
- ⁸C. J. Colyer, S. M. Bellm, B. Lohmann, G. F. Hanne, O. Al-Hagan, D. H. Madison, and C. G. Ning, *J. Chem. Phys.* **133**, 124302 (2010).
- ⁹I. Tóth and L. Nagy, *J. Phys. B* **43**, 135204 (2010).
- ¹⁰K. L. Nixon, A. J. Murray, H. Chaluvadi, C. Ning, and D. H. Madison, *J. Chem. Phys.* **134**, 174304 (2011).
- ¹¹D. S. Milne-Brownlie, M. Foster, J. Gao, B. Lohmann, and D. H. Madison, *Phys. Rev. Lett.* **96**, 233201 (2006).
- ¹²O. Al-Hagan, C. Kaiser, D. Madison, and A. J. Murray, *Nat. Phys.* **5**, 59 (2009).
- ¹³J. P. Doering and J. Yang, *Phys. Rev. A* **54**, 3977 (1996).
- ¹⁴A. Naja, E. M. Staicu-Casagrande, A. Lahmam-Bennani, M. Nekkab, F. Mezdari, B. Joulakian, O. Chuluunbaatar, and D. H. Madison, *J. Phys. B* **40**, 3775 (2007).
- ¹⁵I. Tóth and L. Nagy, *J. Phys. B* **44**, 195205 (2011).
- ¹⁶D. S. Milne-Brownlie, S. J. Cavanagh, B. Lohmann, C. Champion, P. A. Hervieux, and J. Hanssen, *Phys. Rev. A* **69**, 032701 (2004).
- ¹⁷C. Champion, C. D. Cappello, S. Houamer, and A. Mansouri, *Phys. Rev. A* **73**, 012717 (2006).
- ¹⁸K. L. Nixon, A. J. Murray, O. Al-Hagan, D. H. Madison, and C. Ning, *J. Phys. B* **43**, 035201 (2010).
- ¹⁹M. J. Hussey and A. J. Murray, *J. Phys. B* **38**, 2965 (2005).
- ²⁰J. Colgan, M. S. Pindzola, F. Robicheaux, C. Kaiser, A. J. Murray, and D. H. Madison, *Phys. Rev. Lett.* **101**, 233201 (2008).
- ²¹A. Senftleben, O. Al-Hagan, T. Pflüger, X. Ren, D. Madison, A. Dorn, and J. Ullrich, *J. Chem. Phys.* **133**, 044302 (2010).
- ²²D. H. Madison and O. Al-Hagan, *J. At. Mol. Opt. Phys.* **2010**, 367180 (2010).
- ²³K. L. Nixon, A. J. Murray, H. Chaluvadi, S. Amami, D. H. Madison, and C. Ning, *J. Chem. Phys.* **136**, 094302 (2012).
- ²⁴J. Gao, D. H. Madison, and J. L. Peacher, *J. Chem. Phys.* **123**, 204314 (2005).
- ²⁵A. Senftleben, T. Pflüger, X. Ren, B. Najjari, A. Dorn, and J. Ullrich, *J. Phys. B* **45**, 021001 (2012).
- ²⁶X. Ren, A. Senftleben, T. Pflüger, A. Dorn, J. Colgan, M. S. Pindzola, O. Al-Hagan, D. H. Madison, I. Bray, D. V. Fursa, and J. Ullrich, *Phys. Rev. A* **82**, 032712 (2010).
- ²⁷S. Xu, X. Ma, X. Ren, A. Senftleben, T. Pflüger, A. Dorn, and J. Ullrich, *Phys. Rev. A* **83**, 052702 (2011).
- ²⁸J. Ullrich, R. Moshhammer, A. Dorn, R. Dörner, L. P. H. Schmidt, and H. Schmidt-Böcking, *Rep. Prog. Phys.* **66**, 1463 (2003).
- ²⁹W. C. Wiley and I. H. McLaren, *Rev. Sci. Instrum.* **26**, 1150 (1955).
- ³⁰X. Liu and D. E. Shemansky, *J. Geophys. Res.* **111**, A04303, doi:10.1029/2005JA011454 (2006).
- ³¹J. Gao, J. L. Peacher, and D. H. Madison, *J. Chem. Phys.* **123**, 204302 (2005).
- ³²J. Gao, D. H. Madison, and J. L. Peacher, *Phys. Rev. A* **72**, 032721 (2005).
- ³³C. Lee, W. Yang, and R. G. Parr, *Phys. Rev. B* **37**, 785 (1998).
- ³⁴C. F. Guerra, J. G. Snijders, G. T. Velde, and E. J. Baerends, *Theor. Chem. Acc.* **99**, 391 (1998).
- ³⁵S. J. Ward and J. H. Macek, *Phys. Rev. A* **49**, 1049 (1994).
- ³⁶J. B. Furness and I. E. McCarthy, *J. Phys. B* **6**, 2280 (1973).
- ³⁷J. P. Perdew and A. Zunger, *Phys. Rev. B* **23**, 5048 (1981).
- ³⁸N. T. Padial and D. W. Norcross, *Phys. Rev. A* **29**, 1742 (1984).
- ³⁹S. Rioual, A. Pochat, F. Gelebart, R. J. Allan, C. T. Whelan, and H. R. J. Walters, *J. Phys. B* **28**, 5317 (1995).
- ⁴⁰X. Ren, T. Pflüger, J. Ullrich, O. Zatsarinny, K. Bartschat, D. H. Madison, and A. Dorn, *Phys. Rev. A* **85**, 032702 (2012).
- ⁴¹R. F. Frey and E. R. Davidson, *J. Chem. Phys.* **88**, 1775 (1988).